

# IJMC/FEF Student Research Competition



## LOW DISTORTION INTENSIVE QUENCH OF LOW-ALLOY HIGH HARDENABILITY STEEL

Jackson Piontek

Metallurgical Engineering, Missouri University of Science and Technology, Rolla, MO, USA

Copyright © 2022 American Foundry Society  
<https://doi.org/10.1007/s40962-022-00927-1>

### Abstract

*This work aims to compare methods of quenchant delivery between an intensive quench (IQ) system and forced convection bath (FCB) systems. 4340 billets were machined, austenitized, quenched, and examined for distortion. The parts were then sectioned for hardness, and the microstructure was characterized by light optical microscopy. The results show that spray pattern arrangement is critical for effectively quenching the part without distortion*

*or cracking and that the IQ process can be used with more versatility to quench highly hardenable castings without cracking.*

**Keywords:** *quench-hardening, water quenching, intensive quench, forced convection, low-distortion, low-alloy steels, spray quench*

### Introduction

In 2020, an intensive spray quench tank was constructed for use in Missouri S&T's Heat Treatment Lab. An intensive quench system produces first a martensitic shell and austenitic core. Then, the core can be hardened or air cooled, depending on purpose. In addition, the spray quench design allows for greater cost savings, less water usage, and less environmental concerns than that of immersion bath systems. C-rings machined from 4340 were chosen as test castings to reduce variability in grain size and chemistry. The high hardenability of 4340 and the variable section sizes and design of these C-rings make them the ideal candidates to quantify any distortion or stresses caused by the different quenches. By varying the quench orientation in the IQ system, these C-rings should show any cracking, in ways that easily indicate where stresses are present.<sup>1-3</sup>

### Methodology

The 4340 steel in this trial was machined from a single continuously cast 6" square billet. The chemistry was measured using Leco combustion methods for carbon and

sulfur and optical emission spectroscopy (OES) for all other elements. Each quench method was allocated 10 rings to test. The rings for the IQ system are identified as part numbers 51–60, and those quenched in the FCB system were notated 61–70. It should be noted that this is a small part of a large study with several industry partners, which is why the rings were given these numbers.

In preparation for austenitizing and quenching, the rings were welded to rebar at the base to support fitting into the quench systems, and the rings were wrapped in stainless steel foil to prevent scaling during the heating process. Regardless of quenching method, each ring was individually heated to 920 °C for an hour and then quenched in 22–25 °C water for 2.5 min. The IQ system was set to deliver water at 180 psi, while the FCB, which is controlled by velocity, was set to deliver at a velocity of 6 ft/s.

In the FCB system, all 10 rings were quenched with the forks down. In the IQ system, 3 rings were tested with a 45° offset to the nozzles, while the rest were quenched in-plane with the nozzles. This orientation is shown in Figure 1. Transfer time between furnace and quench was also tracked for each quench method.

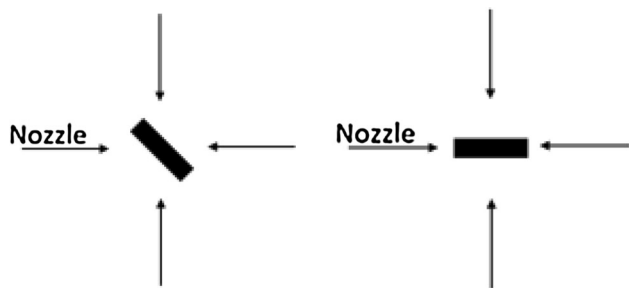


Figure 1. Orientation for IQ spray system, 45° offset (left) and in-plane (right).

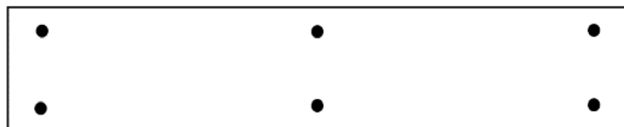


Figure 2. Fork gap point measurements viewed from between forks.

The measurement of distortion and crack failure was done using the gap between the forks of the C-rings, which, if measured in multiple places, can give an indication to the direction of change in shape of the C-ring. This is shown in more detail in Figure 2. The gap was measured in 6 places, before and after quenching, and the percent change for each ring was established.

After distortion measurement, samples were sectioned for hardness testing using Rockwell C scale and light optical microscopy (LOM). The sectioning procedure is shown in Figure 3. Hardness testing was measured as an average for each sample, with maps produced for individual hardness measurements in relation to location in the sample. An average can be computed because through-hardening should be produced in both methods. The LOM samples were etched with a 2% Nital solution.

## Results and Discussion

### Chemistry

The chemistry results, shown in Table 1, show slightly high levels of manganese and chrome when compared to 4340 standards. Because this study is comparative between quenchant delivery methods, this will not negatively affect

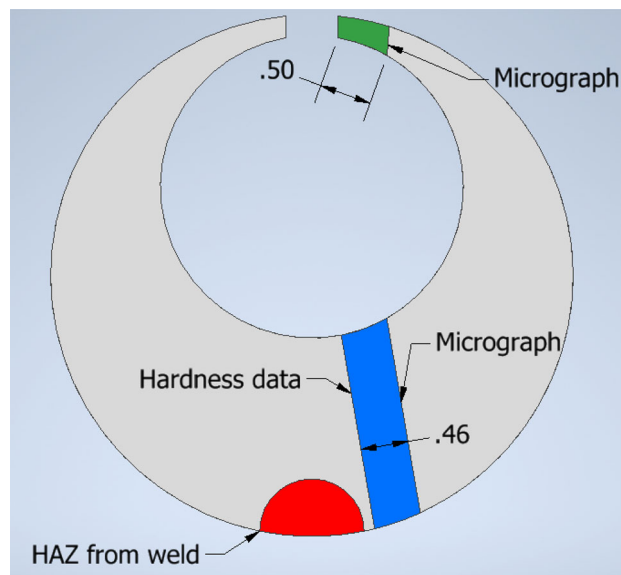


Figure 3. Sectioning procedure for C-rings.

other testing data. Also, as the goal is to minimize distortion in high hardenability steels, the Mn and Cr levels contribute to a larger ideal diameter, DI, for martensite formation and further validate any testing results.

### Hardness and Transfer Time

The FCB system produced a transfer time between 7 and 12 s for all 10 samples. While this is slightly higher than desired, the samples were insulated with refractory blanket during transfer to reduce cooling before quench. The samples tested for hardness produced an average hardness of  $57 \pm 1$  HRC.

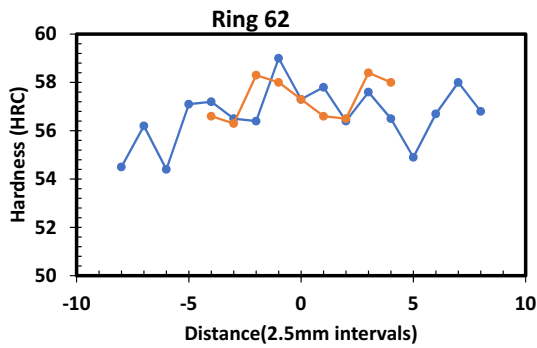
In comparison, the IQ system produced a shorter transfer time of  $< 7$  s for all 10 samples, simply due to space allocation in each testing room. Hardness testing showed a more consistent through-hardness of  $58 \pm 1$  HRC. Maps of the hardness based on orientation for one FCB and one IQ sample are shown in Figures 4 and 5.

### Distortion and Stress-Induced Cracking

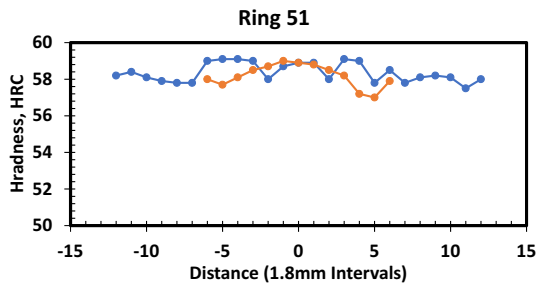
Only one sample quenched in FCB failed as a result of quench stress. However, this one cracked sample was

Table 1. Chemistry Results from OES and Leco C-S Testing

Element	C	Si	Mn	P	S	Cr	Mo	Ni	Al	Cu	Ti	V
Wt%	0.408	0.163	0.859	0.0545	0.0074	1.06	0.3	1.69	0.036	0.214	0.006	0.029



**Figure 4. Hardness map for FCB sample, ring 62. Orange line represents thickness direction, and blue line represents height direction.**



**Figure 5. Hardness map for IQ sample, ring 51. Orange line represents thickness direction, and blue line represents height direction.**



**Figure 6. Crack in ring 57, another crack is present with 180° symmetry to this crack.**

caused by improper placement in the FCB tank. For the other 9 samples, the distortion was minimal with every fork gap measurement falling below 3% change due to quenching. This will be the control used for comparison in the IQ system.



**Figure 7. Crack in ring 55. Unlike ring 57, there is not a symmetrical crack present.**

All 7 IQ samples quenched in-plane with the nozzles produced visible distortion, with 4 cracking in various ways. The fork gap measurements all fell between 3 and 5% distortion. The placement of the cracking on the sample seemed to change with even minute changes of quench orientation. For example, if a ring was quenched in the IQ system slightly offset from in-plane, around 5–10°, the ring would manifest cracking along the “mid-radius” of the fork, with the cracks typically appearing in symmetry. This is what occurred to ring 57, which is shown in Figure 6. If a ring was placed nearly, or exactly in plane, < 5° offset, the cracking would manifest across the fork at around the middle of the fork height. It is speculated this is due to the high concentration of quenchant at this point, causing a fully martensitic “bridge” to the inner radius of the sample, which acting as a point of tension during the cooling of the part above and below this point. This is shown in detail in Figure 7. Within the samples that were not cracked, the distortion tended to show in the same orientation-dependent manner. When a ring was placed slightly off axis, the forks would become misaligned, protruding along the axis of the thickness. However, when placed in-plane, the ring would distort by “opening” or “closing” the gap perpendicular to the thickness.

The rings quenched at 45° offset to the nozzles showed much less distortion than those quenched in plane. The fork gap changes ranged from 0.5 to 3%, which is in line with that of the FCB testing. One of the rings showed visible distortion in a similar manner to the slightly misaligned rings from the in-plane set, with the forks misaligning along the thickness axis. Lastly, the offset orientation seems to be more forgiving to slight changes in angle from the nozzle. This is most likely due to the slightly increased

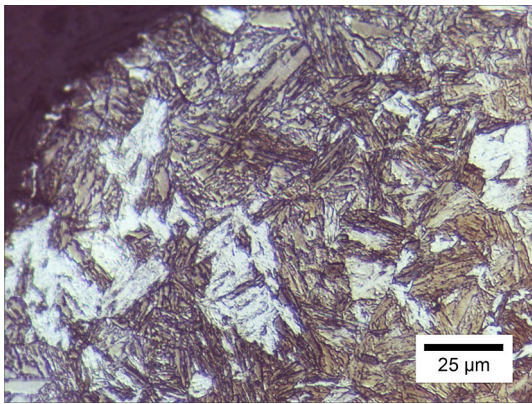


**Figure 8.** LOM image of base of ring 62, showing about 200  $\mu\text{m}$  of decarburization due to loose steel wrap.

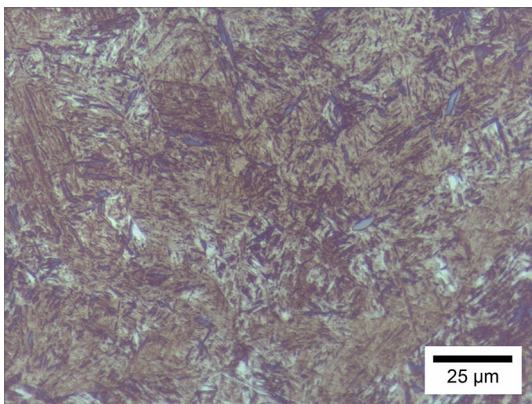


**Figure 9.** LOM image of base of ring 51, showing about 350  $\mu\text{m}$  of decarburization due to loose steel wrap.

distance between the nozzle and ring, causing a larger spray pattern and a larger zone of coverage for water spray.

### LOM Analysis

The microstructure of the sectioned samples showed a martensitic structure, with minimal change between quenchant methods. This is expected as the DI of 4340 is greater than 2". MnS inclusions were found, which is typical for a steel of this grade. Slight decarburization occurred, with a higher decarburization depth near the base of the sample, shown in Figures 8 and 9. This is likely caused by small gaps in the stainless steel wrap near the base of the sample, where the fitting bar was attached.

### Conclusions

In this study, an examination of quenchant delivery was conducted using 4340 C-rings. An FCB system, used as a control, was compared to two different orientations in an IQ spray system. The two orientations, in-plane and 45°

offset, produced different amounts and types of distortion. In-plane quenching produced higher distortion than the FCB system, with a crack rate of over 50%. Points of cracking and distortion of these parts also highly depended on whether the part was perfectly aligned in-plane with the nozzles. The rings quenched offset to the nozzles distorted much less, showing no cracking and similar distortion measurements to that of the FCB system.

### Current and Future Work

Work is currently in progress to characterize whether these phenomena described to this point change with the added stress of mechanical defects in these parts. Work is also being completed on directly cast rings as opposed to machined specimens.

### Acknowledgements

The authors greatly appreciate support for this research from DLA-Troop Support, Philadelphia, PA and the Defense Logistics Agency Information Operations, J68, Research & Development, Ft. Belvoir, VA. Nucor Inc. is also greatly appreciated for contribution of the 4340 billet material.

### REFERENCES

1. E. Boyle, R. Bowers, D.O. Northwood, The use of navy C-ring specimens to investigate the effects of initial microstructure and heat treatment on the residual stress, retained austenite, and distortion of carburized automotive steels. *SAE Trans. J. Mater. Manuf.* **116**, 253–261 (2007)
2. C. Nan, D.O. Northwood, R.J. Bowers, X. Sun, P. Bauerle, Residual stresses and dimensional changes in ferritic nitrocarburized navy C-rings and prototype stamped parts made from SAE 1010 steel. *SAE Int. J. Mater. Manuf.* **2**(1), 219–233 (2009)
3. D.O. Northwood, R.J. Bowers, A. Clark, Heat treatment effects on distortion, residual stress, and retained austenite in carburized 4320 steel. *Mater. Sci. Forum* **783–786**, 692–697 (2014)

**Publisher's Note** Springer Nature remains neutral with regard to jurisdictional claims in published maps and institutional affiliations.

Springer Nature or its licensor (e.g. a society or other partner) holds exclusive rights to this article under a publishing agreement with the author(s) or other rightsholder(s); author self-archiving of the accepted manuscript version of this article is solely governed by the terms of such publishing agreement and applicable law.